Table S1. Ophthalmological data of the four affected patients from three unrelated families

	First symptom Age of onset	**First exam** Age Visual acuity Visual field	**Last exam** Age Visual acuity Visual field	**Refraction**	**Final SD-OCT**	**Final SW-FAF**	**ERG**
Patient 1 Family 1 French	Night blindness Childhood	12 years **RE** 6/10 **LE** 5/10 No peripheral constriction	19 years **RE** 6/10, **LE** 5/10 **RE** = 30° (T,N,I,S) **LE** = 30° (T,N,I,S)	**RE** -3 (-2 at 20°) **LE** -5 (-3 at 175°)	Large macular preservation	Subtle large annular ring Hypoautofluorescent atrophic spots in the mid periphery of the retina	Rod and cone responses not discernable
Patient 2 Family 2 Italian	Night blindness Childhood	34 years **RE** 9/10 **LE** 9/10	36 years **RE** 9/10, **LE** 9/10 **RE** 20° (T), 35° (N), 20° (I), 10° (S) **LE** 10°(T), 15°(N), 20° (I), 10°(S)	**RE** -7.25 (-2.75 at 10°) **LE** -6.75 (-2.75 at 180°)	Central island of preserved retinal architecture Gradual disappearance of outer retinal layers with increasing eccentricity	Hyperautofluorescent perifoveal ring Multiple peripheral hypoautofluorescent spots beyond the temporal vascular arcades	Rod and cone responses not discernable
Patient 3 Family 3 Spanish	Night blindness 20 years	25 years N/A	54 years **RE** 1/10, **LE** 1/20 Tunnel vision **RE** 5°, LE 10°	**RE** +0.25 (-0.75 at 39°) **LE** +1.25 (-1.25 at 50°)	Atrophy with thinning of the retinal neuroepithelium also affecting the central retina	N/A	Rod and cone responses not discernable
Patient 4 Family 3 Spanish	Night blindness 20 years	30 years	59 years **RE** 1/10, **LE** 1/10 Tunnel vision **RE** 5°, **LE** 10°	**RE** +6.5 (-1.25 at 35°) **LE** +6 (-1.25 at 150°)	Atrophy with thinning of the retinal neuroepithelium also affecting the central retina	N/A	Rod and cone responses not discernable

ERG – electroretinogram; T – temporal, N – nasal, I – inferior, S – superior; N/A – not available

Table S2. *Xenopus* morpholino and primer sequences

Morpholino	Sequence
Tbc1d32-MO-1	TTTTTGACGGGACGGTCCAGATTTT
Tbc1d32-MO-2	CTTCAAAGGCAGCGTCGCCCAAGAG
Standard control-MO	CCTCTTACCTCAGTTACAATTTATA
Tbc1d32 forward	TCAAGGCCT-CTCGAG-ATG-TCTCATTTTTCTTCTGAG
Tbc1d32 reverse	GTTCTAGAGG-CTCGAG-TCA-TTGTATTACAGAG

Table S3. Human *TBC1D32* gDNA amplification and sequencing primer sequences

Target	Experiment	Forward primer	Reverse primer
TBC1D32	Amplification exon 2	TAACCTGCTGAAGTTTGGGC	AAGCCTTTGGAGAGTCTGGG
	Amplification exon 7	TCTCTATTCTATTCTTGTGAGA	ATGGAGCTTCTTTCTGATA
	Sequencing exon 2		AAGCCTTTGGAGAGTCTGGG
	Sequencing exon 7	TCTCTATTCTATTCTTGTGAGA	
	Amplification & sequencing exon 1	TTCTCTGGACCCTCTCTGGA	GTTTTCCGAAATGACGCACT
	Amplification & sequencing exon 11	ACAGCATCATTAGTAAAAGTGACCT	GGCTGAGCTTTAAGGGCTAGA

Table S4. *Xenopus* and human RT-PCR and/or qPCR primer sequences

Xenopus target	Experiment	Forward primer	Reverse primer
ef1a	qPCR	TGGTGGCATCGACAAGAGAAC	CCACGTTCACGCTCTGCCTTC
ihh	qPCR	GCAGTCGACATCACCACATC	CTGACTTCACCGAGCAATGG
mitf	qPCR	CATTAACGTCTCCAGCAGCC	TGTTTGGCCGTAGTCAGGTA
odc	qPCR	GCTTCTGGAGCGGGCAAAGGA	CCAAGCTCAGCCCCCATGTCA
rpl8	qPCR	CCACGTGTCCGTGGTGTGGCTA	GCGCAGACGACCAGTACGACGA
tbc1d32	qPCR	GGAGGCAATGCAAACACTCT	CCGCAAAATCCGCTCTGTAA

Human target	Experiment	Forward primer	Reverse primer
TBC1D32	RT-PCR exons 1-5	GGCCCATTTCTCCAGCGA	ATCCGGTCACTAAACACAGG
	RT-PCR exons 1-8	GGCCCATTTCTCCAGCGA	CTCTGGATGACGAATCCAGAAAG
	RT-PCR exons 6-11	CTCTGCGAAAAACTGACCGTG	TCTGCTTGTTTCTGCAATGCT
	RT-PCR exons 10-12	TGGATGCATGCACATTATAGC	TGAGGGATACCAAACCTTTTT
	qPCR	TGCCACCCCCAAAGGATTAC	TTAGTGCAATGCCACCTGCT
ZO1	qPCR	TAAGCCAGCCTCTCAACAGAA	AGAGGTGGAAGGAGCTGGG
MERTK	qPCR	CTGCAGCTAGAAAAACTCTT	GAGGCAATTATAGAGTCAGG
LRAT	qPCR	AAACCAGCTCTTTCCACCGA	TGAGACGCTTGTTGGAGACC
RPE65	qPCR	TCTTTGCAACTATGTCTCTG	TTATTGGATCTTCCTTGTCT
ABCA4	qPCR	AGCCATGTTGGAGGACACAG	AGCAGATCCCAGATTGAGCG
RLBP1	qPCR	GAAATCACCTTTGATGAGAT	TCTTCCTGAGATCTGAAGTC
CDH1	qPCR	CGGACGATGATGTGAACACC	TTGCTGTTGTGCTTAACCCC
CDH2	qPCR	CGGTTTCATTTGAGGGCACA	TTGGAGCCTGAGACACGATT
CDH3	qPCR	GAAGCTGGCAGACATGTACG	AAGCCACCACTCTAACGTCA
CTNNB1	qPCR	CTTACACCCACCATCCCACT	CCTCCACAAATTGCTGCTGT
FN1	qPCR	CCCCATTCCAGGACACTTCT	TGCCTCCACTATGACGTTGT
SNAI1	qPCR	AGTGGTTCTTCTGCGCTACT	GTAGGGCTGCTGGAAGGTAA
NANOG	qPCR	CAAAGGCAAACAACCCACTT	TCTGCTGGAGGCTGAGGTAT
OCT3/4	qPCR	GTACTCCTCGGTCCCTTTCC	CAAAAACCCTGGCACAAACT
LIN28a	qPCR	GGGGAATCACCCTACAACCT	CTTGGCTCCATGAATCTGGT
GAPDH	qPCR	AACCATGAGAAGTATGACAAC	CTTCCACGATACCAAAGTT

Table S5: *Xenopus* primary and secondary antibodies

Primary antibodies	Host	Clonality	Dilution	Company	Catalogue #
anti-acetylated alpha-Tubulin	Mouse	Monoclonal	1/500	Sigma-Aldrich	T6793
anti-Arl13B	Rabbit	Polyclonal	1/200	Proteintech	17711-1-AP
anti-cleaved Caspase 3	Rabbit	Polyclonal	1/200	Cell signaling	9661S
anti-gamma-Tubulin	Mouse	Monoclonal	1/200	Anticorps-enligne.fr	ABIN207111
anti M-Opsin	Rabbit	Polyclonal	1/500	Sigma-Aldrich	AB5405
anti-S-Opsin	Rabbit	Polyclonal	1/500	Sigma-Aldrich	AB5407
anti-Otx2	Rabbit	Monoclonal	1/100	Abcam	AB183951
anti-Rhodopsin	Mouse	Monoclonal	1/1000	Sigma-Aldrich	MABN15

Secondary antibodies	Host	Dilution	Company	Catalogue #
anti-mouse IgG Alexa Fluor 488	Goat	1/1000	ThermoFisher Scientific	A11001
anti-mouse IgG1 Alexa Fluor 488	Goat	1/300	ThermoFisher Scientific	A21121
anti-rabbit IgG Alexa Fluor 488	Goat	1/1000	ThermoFisher Scientific	A11008
anti-rabbit IgG Alexa Fluor 546	Goat	1/300	ThermoFisher Scientific	A11010
anti-mouse IgG Alexa Fluor 594	Goat	1/1000	ThermoFisher Scientific	A11005
anti-rabbit IgG Alexa Fluor 594	Goat	1/1000	ThermoFisher Scientific	A11012
anti-mouse IgG Alexa Fluor 647	Goat	1/500	ThermoFisher Scientific	A21240

Table S6: Human primary and secondary antibodies

Primary antibodies	Host	Clonality	Dilution	Company	Cat #
anti-ABCA4, clone 3F4	Mouse	Monoclonal	1/200	Abcam	ab77285
anti-acetylated alpha-Tubulin, clone 6-11B-1	Mouse	Monoclonal	1/2000	Sigma-Aldrich	T7451
anti-AFP, clone 1G7	Mouse	Monoclonal	1/200	Sigma-Aldrich	WH0000174M1
anti-ARL13B	Rabbit	Polyclonal	1/3000	Proteintech	17711-1-AP
anti-β-actin, clone AC-74	Mouse	Monoclonal	1/500 (WB)	Sigma-Aldrich	A5316
anti-Arrestin 3	Goat	Polyclonal	1/200	Novus Biologicals	NBP1-37003
anti-β-catenin, clone 14	Mouse	Monoclonal	1/1000 (WB)	BD Transduction Laboratories	610154
anti-CRALBP, clone B2	Mouse	Monoclonal	1/1000	Abcam	ab15051
anti-CRALBP	Rabbit		1/1000 (WB)	Proteintech	
anti-CRX, clone 4G11	Mouse	Monoclonal	1/2000	Abnova	H00001406-M02
anti-E-cadherin, clone 2410E	Rabbit	Monoclonal	1/1000 (WB)	Cell Signaling Technology	3195
anti-GAFP	Rabbit	Polyclonal	1/200	Agilent Dako	Z0334
anti-GRK1, clone G8	Mouse	Monoclonal	1/500	ThermoFisher Scientific	MA1-720
anti-GT335	Mouse	Monoclonal	1/2000	AdipoGen	AG-20B-0020
anti-IFT88	Rabbit	Polyclonal	1/500	Proteintech	13967-1-AP
anti-MERTK, clone Y323	Rabbit	Monoclonal	1/250	Abcam	ab52968
anti-Nanog	Rabbit	Polyclonal	1/200	Abcam	ab21624
anti-N-cadherin, clone D4R1H	Rabbit	Monoclonal	1/200 1/1000 (WB)	Cell Signaling Technology	13116
anti-OCT3/4, clone C-10	Mouse	Monoclonal	1/200	Santa Cruz Biotechnology	sc-5279
anti-Opsin red/green	Rabbit	Polyclonal	1/500	Millipore	AB5405
anti-P-cadherin, clone 56	Mouse	Monoclonal	1/250 (WB)	BD Transduction Laboratories	610228
anti-PDE6B	Rabbit	Polyclonal	1/1000	Proteintech	22063-1-AP
anti-Perilipin-2	Guinea Pig	Polyclonal	1/1000 (WB)	Progen	GP47
anti-Pericentrin	Mouse	Monoclonal	1/1000	Abcam	ab28144
anti-Recoverin	Rabbit	Polyclonal	1/2000	Millipore	AB5585
anti-Rhodopsin, clone 4D2	Mouse	Monoclonal	1/500	Millipore	MABN15
anti-SMA, clone 1A4	Mouse	Monoclonal	1/200	Agilent Dako	M0851
anti-SOX2	Rabbit	Polyclonal	1/200	ThermoFisher Scientific	48-1400
anti-TBC1D32	Rabbit	Polyclonal	1/200	Novus Biologicals	NBP1-90777
anti-vimentin, clone V9	Mouse	Monoclonal	1/100	Dako Gifted by C. Crozet (INM, Montpellier, France)	M0725
anti-ZO-1, clone 1A12	Mouse	Monoclonal	1/500	ThermoFisher Scientific	33-9100
anti-ZO-1	Rabbit	Polyclonal	1/100	ThermoFisher Scientific	40-2200

Secondary antibodies	Host	Dilution	Company	Cat #
anti-Goat IgG Alexa Fluor 594	Donkey	1/500	ThermoFisher Scientific	A-11058
anti-Mouse IgG Alexa Fluor 488	Donkey	1/500	ThermoFisher Scientific	A-21202
anti-Mouse IgG Alexa Fluor 594	Donkey	1/500	ThermoFisher Scientific	A-21203
anti-Rabbit IgG Alexa Fluor 488	Donkey	1/500	ThermoFisher Scientific	A-21206
anti-Rabbit IgG Alexa Fluor 594	Donkey	1/500	ThermoFisher Scientific	A-21207
anti-Mouse IgG Alexa Fluor 488 AffiniPure	Donkey	1/500	Jackson ImmunoResearch	715-546-151
anti-Rabbit IgG Alexa Fluor 488 AffiniPure	Donkey	1/500	Jackson ImmunoResearch	711-545-152
anti-Mouse IgG IRDye 680RD	Donkey	1/20000 (WB)	LI-COR Biosciences	926-68072
anti-Rabbit IgG IRDye 800CW	Donkey	1/20000 (WB)	LI-COR Biosciences	926-32213
anti-Guinea pig IRDye 800CW	Donkey	1/20000 (WB)	LI-COR Biosciences	926-32411

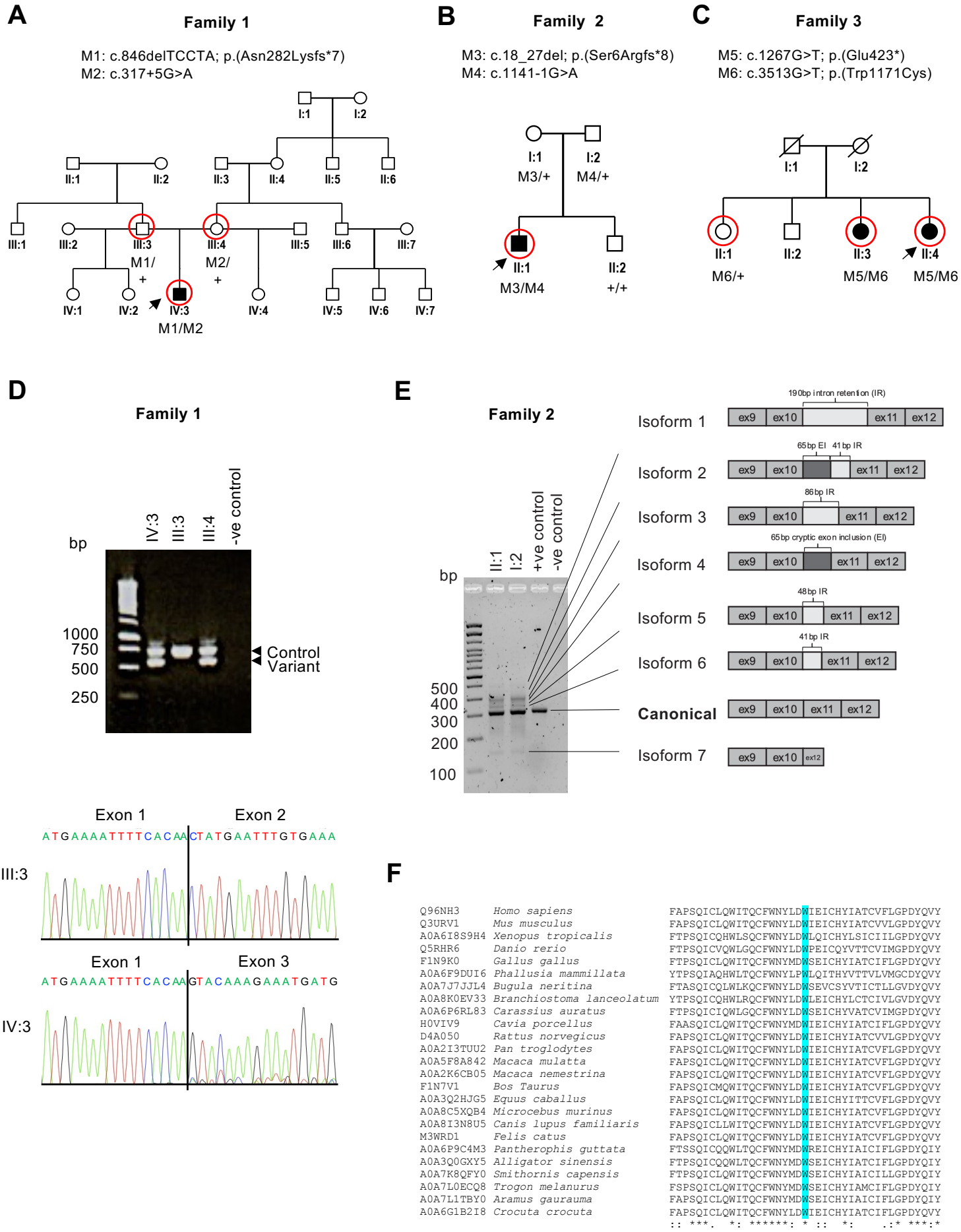
A
Family 1
M1: c.846delTCCTA; p.(Asn282Lysfs*7)
M2: c.317+5G>A
I:1
I:2
II:1
II:2
II:3
II:4
II:5
II:6
III:1
III:2
III:3
III:4
III:5
III:6
III:7
M1/+
M2/+
IV:1
IV:2
IV:3
IV:4
IV:5
IV:6
IV:7
M1/M2
B
Family 2
M3: c.18_27del; p.(Ser6Argfs*8)
M4: c.1141-1G>A
I:1
M3/+
I:2
M4/+
II:1
M3/M4
II:2
+/+
C
Family 3
M5: c.1267G>T; p.(Glu423*)
M6: c.3513G>T; p.(Trp1171Cys)
I:1
I:2
II:1
M6/+
II:2
II:3
M5/M6
II:4
M5/M6
D
Family 1
bp
IV:3
III:3
III:4
-ve control
1000
750
500
250
Control
Variant
Exon 1
Exon 2
ATGAAAATTTTCACAACTATGAATTTGTGAAA
III:3
Exon 1
Exon 3
ATGAAAATTTTCACAAGTACAAAGAAATGATG
IV:3
E
Family 2
bp
II:1
I:2
+ve control
-ve control
500
400
300
200
100
190bp intron retention (IR)
Isoform 1
ex9
ex10
ex11
ex12
65bp EI
41bp IR
Isoform 2
86bp IR
Isoform 3
65bp cryptic exon inclusion (EI)
Isoform 4
48bp IR
Isoform 5
41bp IR
Isoform 6
Canonical
Isoform 7
F
Q96NH3 Homo sapiens FAPSQICLQWITQCFWNYLDWIEICHYIATCVFLGPDYQVY
Q3URV1 Mus musculus FAPSQICLQWITQCFWNYLDWIEICHYIATCVVLGPDYQVY
A0A6I8S9H4 Xenopus tropicalis FTPSQICQHWLSQCFWNYLDWLQICHYLSICIILGPDYQVY
Q5RHR6 Danio rerio FTPSQICVQWLGQCFWNYLDWPEICQYVTTCVIMGPDYQVY
F1N9K0 Gallus gallus FTPSQICLQWITQCFWNYMDWSEICHYIATCIFLGPDYQVY
A0A6F9DUI6 Phallusia mammillata YTPSQIAQHWLTQCFWNYLPWLQITHYVTTVLVMGCDYQVY
A0A7J7JJL4 Bugula neritina FTASQICQLWLKQCFWNYLDWSEVCSYVTICTLLGVDYQVY
A0A8K0EV33 Branchiostoma lanceolatum YTPSQICQHWLRQCFWNYLDWLEICHYLCTCIVLGVDYQVY
A0A6P6RL83 Carassius auratus FTPSQICIQWLGQCFWNYLDWSEICHYVATCVIMGPDYQVY
H0VIV9 Cavia porcellus FAASQICLQWITQCFWNYMDWIEICHYIATCIFLGPDYQVY
D4A050 Rattus norvegicus FAPSQICLQWITQCFWNYLDWIEICHYIATCVVLGPDYQVY
A0A2I3TUU2 Pan troglodytes FAPSQICLQWITQCFWNYLDWIEICHYIATCVFLGPDYQVY
A0A5F8A842 Macaca mulatta FAPSQICLQWITQCFWNYLDWIEICHYIATCVFLGPDYQVY
A0A2K6CB05 Macaca nemestrina FAPSQICLQWITQCFWNYLDWIEICHYIATCVFLGPDYQVY
F1N7V1 Bos Taurus FAPSQICMQWITQCFWNYLDWIEICHYIATCVFLGPDYQVY
A0A3Q2HJG5 Equus caballus FAPSQICLQWITQCFWNYLDWIEICHYITTCVFLGPDYQVY
A0A8C5XQB4 Microcebus murinus FAPSQICLQWITQCFWNYLDWIEICHYIATCVFLGPDYQVY
A0A8I3N8U5 Canis lupus familiaris FAPSQICLLWITQCFWNYLDWIEICHYIATCVFLGPDYQVY
M3WRD1 Felis catus FAPSQICLQWITQCFWNYLDWIEICHYIATCVFLGPDYQVY
A0A6P9C4M3 Pantherophis guttata FTSSQICQQWLTQCFWNYMDWREICHYIAICIFLGPDYQIY
A0A3Q0GXY5 Alligator sinensis FTPSQICQQWLTQCFWNYMDWSEICHYIATCIFLGPDYQIY
A0A7K8QFY0 Smithornis capensis FTPSQICLQWITQCFWNYMDWSEICHYIAICILLGPDYQIY
A0A7L0ECQ8 Trogon melanurus FSPSQICLQWITQCFWNYMDWSEICHYIAMCIFLGPDYQIY
A0A7L1TBY0 Aramus guarauna FAPSQICLQWITQCFWNYMDWSEICHYIAICIFLGPDYQIY
A0A6G1B2I8 Crocuta crocuta FAPSQICLQWITQCFWNYLDWIEICHYIATCIFLGPDYQVY

Supplemental Figure 1. Segregation of *TBC1D32* variants in the three families. A-C) Pedigrees of the three families carrying *TBC1D32* variants. Open squares and circles represent healthy males and females, respectively; black squares and circles represent affected males and females, respectively; diagonal lines represent deceased individuals; Roman numerals denote the generation number, and Arabic numerals denote the individuals within a generation. Arrows indicate the probands and red circles indicate the individuals for whom WES was performed. **A**) Family 1 is of French origin. Patient 1 (IV:3) is compound heterozygous for the indel variant M1 and the splice variant M2 (M1/M2). The father (III:3) is a carrier of the indel variant (M1/+) and the mother (III:4) is a carrier of the splicing variant (M2/+). **B**) Family 2 is of Italian origin. Patient 2 (II:1) is compound heterozygous for the indel variant M3 and splicing variant M4 (M3/M4), and the unaffected brother (II:2) carries two wild type alleles (+/+). **C**) Family 3 is of Spanish origin. The affected sisters, Patients 3 and 4 (II:3 and II:4), are compound heterozygous for the nonsense variant M5 and the missense variant M6 (M5/M6), whereas the unaffected sister (II:1) carries only the missense variant (M6/+). **D**) RT-PCR analysis of RNA from Patient 1 (IV:3) and his parents (III:3 and III:4) using primers in exons 1 and overlapping the junction of exons 5 and 6 to evaluate the impact of the *TBC1D32* splicing variant M2. The upper band represents the control allele, and the lower band represents the M2 allele. Sequencing electropherograms showing the exon 1 and 2 junction following RT-PCR analysis of individual III:3 (who does not carry the M2 variant) and the exon 1 and 3 junction in the proband IV:3 due to exon 2 skipping. The vertical line represents the beginning of the divergent sequences between the proband and his father. **E**) RT-PCR analysis of RNA isolated from Patient 2 (II:1), his father (I:2), and a control, using primers overlapping the junction of exons 9 and 10 (forward) and exons 12 and 13 (reverse), to analyze the effect of the M4 variant. A single amplicon of 310 bp, corresponding to the canonical splicing form, is observed in the control sample. A similarly-sized amplicon, as well as longer and shorter amplicons, were observed in the patient and his father, corresponding to the 7 aberrant splicing isoforms promoted by M4. **F**) Alignment of the orthologous sequences of the Rab GAP TBC domain on either side of the Trp residue at position 1171 (highlighted in blue), which is altered by the missense variant in family 3, showing the high degree of amino acid conservation across species. From the left to the right column: accession number, species name, and amino-acid sequence. * indicates a conserved residue, : indicates amino-acids with highly similar properties, and . indicates poorly-conserved amino-acids.

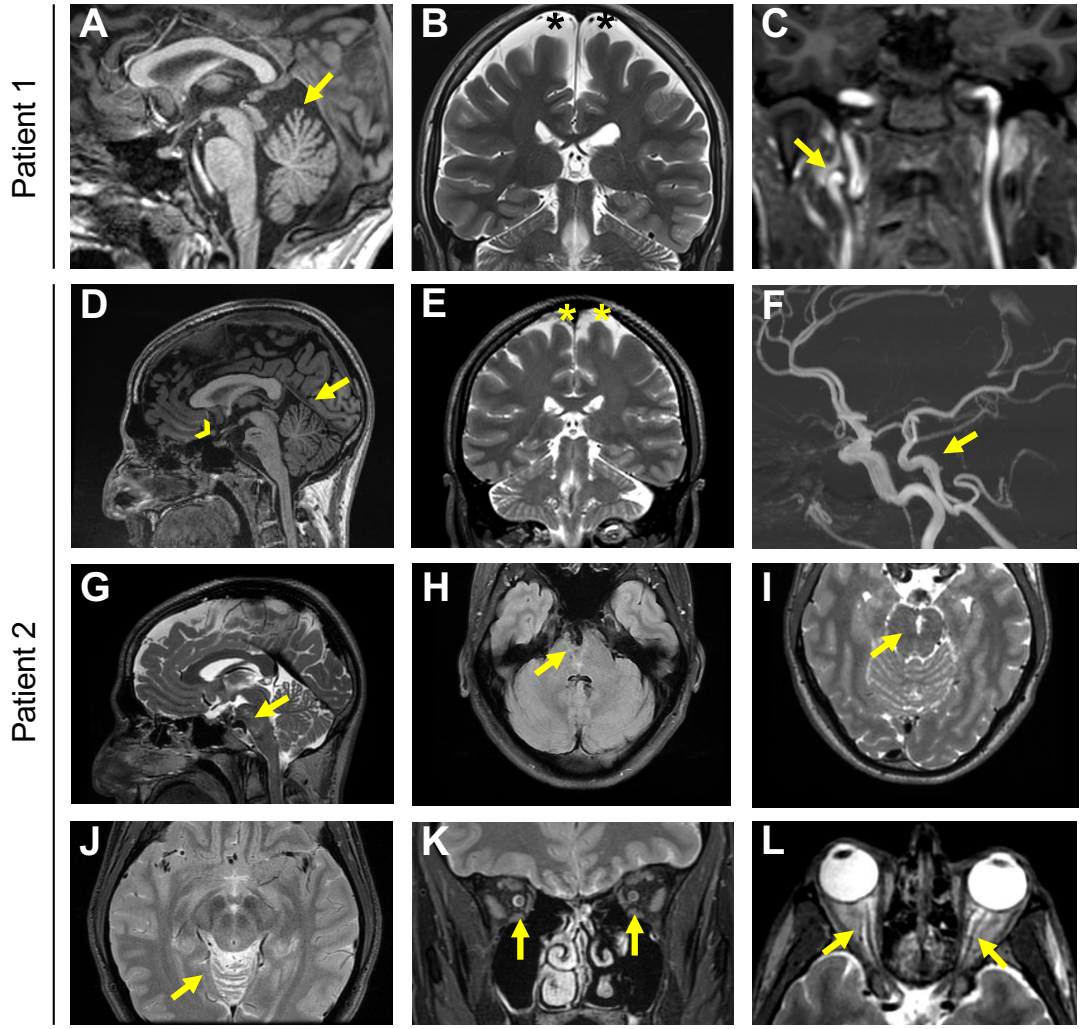

Supplemental Figure 2. Cerebral MRI of Patients 1 and 2. A) Sagittal T1 weighted MRI images showing cerebellar atrophy involving specifically the superior part of the cerebellar vermis (arrow). The pituitary gland is normal both for the anterior and the posterior part. **B**) Coronal T2 weighted images showing diffuse widened subarachnoid spaces suggesting mild cerebral atrophy (black asterisks). **C**) Coronal T1 weighted imaging showing loop of the cervical segment of the right internal carotid artery, which is an unusual finding in young adults (arrow). **D**) Sagittal T1-weighted images showing cerebellar atrophy involving specifically the superior part of the cerebellar vermis (arrow). The pituitary gland is normal both for the anterior and the posterior part (arrowhead). **E**) Coronal T2 weighted images showing diffuse widened subarachnoid spaces suggesting mild cerebral atrophy (asterisks). **F**) 3D Time of Flight images showing the dolichoectasia of the basilar artery (arrow). **G**) Sagittal T2 weighted images showing the slight brainstem compression (arrow). **H**) Axial Fluid Attenuated Inversion Recovery T2 weighted images showing the dolichoectasic basilar trunk in a mid-pons cleft (arrow). **I**) Axial T2 weighted images showing stretched enlarged perivascular spaces in the mid-pons (arrow). **J**) Axial T2 weighted images showing the atrophic superior vermis (arrow). Coronal (**K**) and axial (**L**) T2 weighted images showing bilaterally enlarged perioptic fluid space in the intraconic and pre-bulbar tracts (arrows).

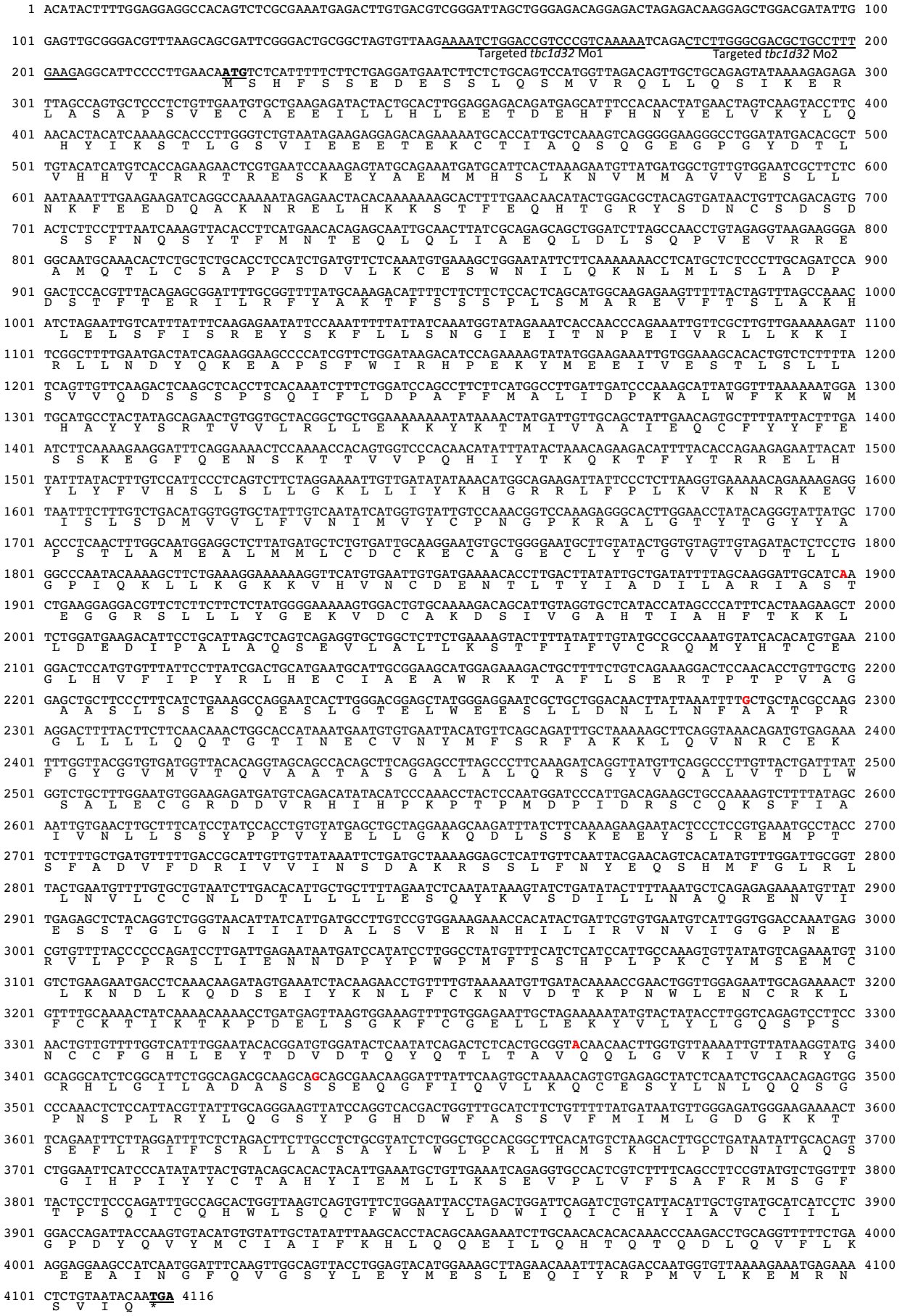

Supplemental Figure 3. *Xenopus tbc1d32* cDNA. The *Xenopus laevis tbc1d32* cDNA was cloned by RT-PCR from *Xenopus* embryo RNA extracts. The start and stop codons are in bold and underlined. Targeted sequences of each *tbc1d32* morpholino are underlined. The predictive protein sequence is indicated under the coding sequence. In red are indicated mismatches with the *Xenopus laevis tbc1d32* predictive sequence of the NCBI EST database (accession # XM_041562734.1).

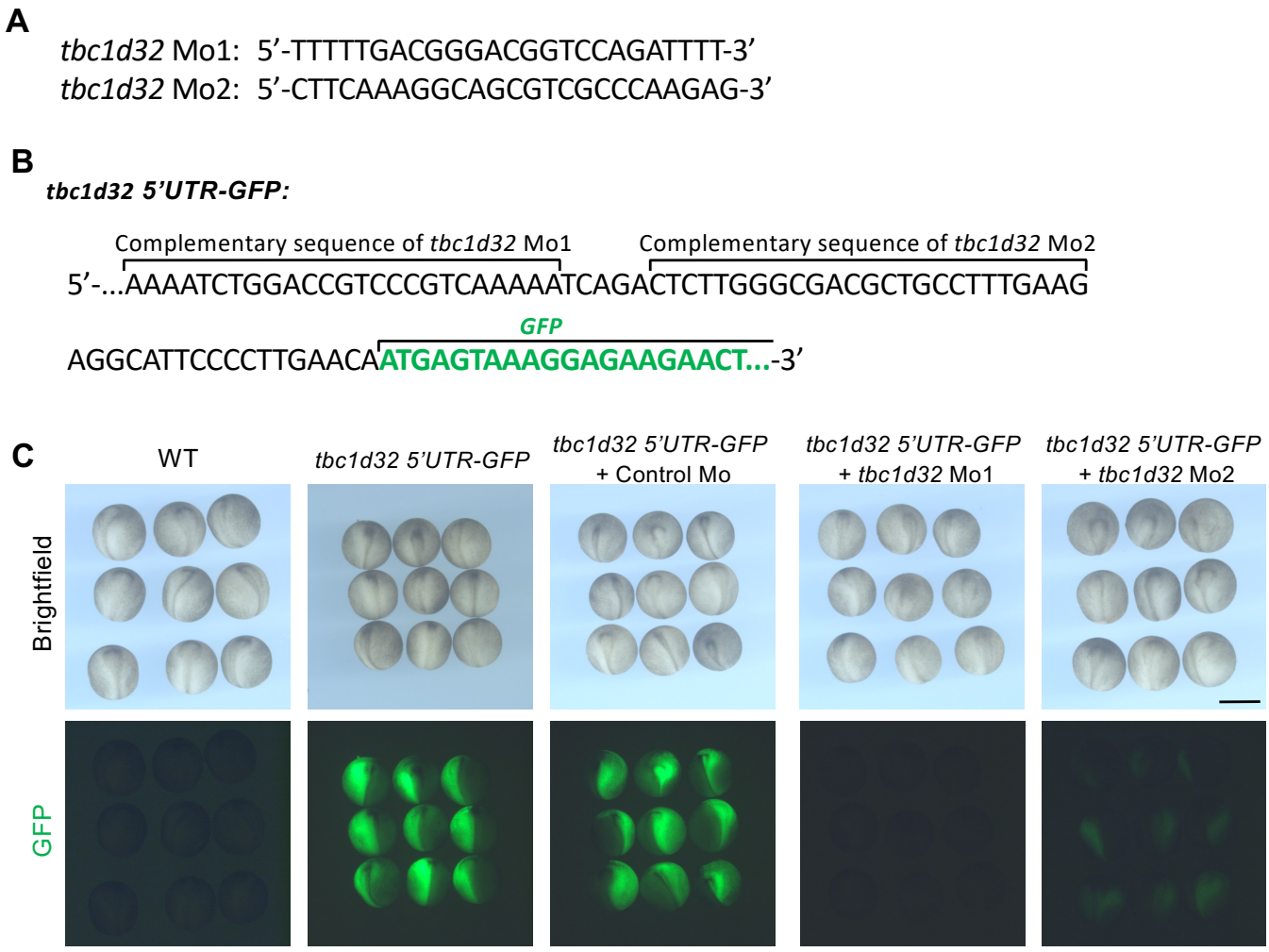

Supplemental Figure 4. *In vivo* validation of *tbc1d32* Mo efficiency. A) Sequences of both *tbc1d32* morpholinos (Mo). **B)** Schematic representation of the chimeric constructs containing a *GFP* sequenced fused downstream of the *tbc1d32* 5'UTR containing the Mo-complementary sequences [*tbc1d32* 5'UTR-GFP]. **C)** *In vivo* GFP fluorescence was analyzed at stage 19 following co-injection of the indicated Mo and *GFP* mRNA constructs. Upper panels: brightfield images of the embryos. *tbc1d32* Mo1 and *tbc1d32* Mo2 inhibited GFP translation from *tbc1d32* 5'UTR-GFP construct, whereas the control Mo did not. Scale bar = 1 mm.

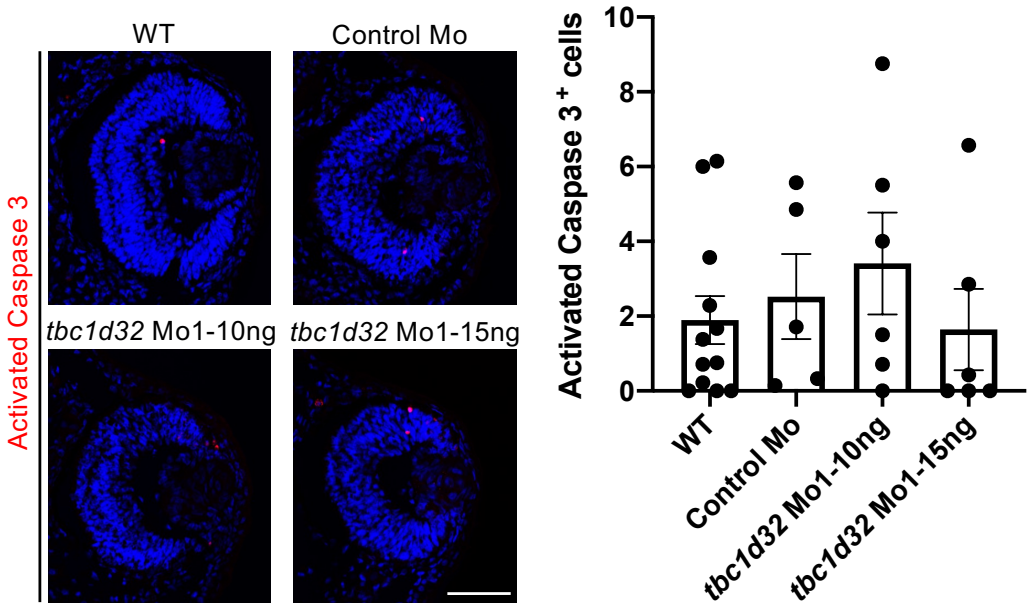

Supplemental Figure 5. Cell death assay in *Xenopus* embryos following *tbc1d32* Mo injections. Activated caspase 3 immunolabelling on retinal sections of wild type embryos (WT), control embryos injected with a standard Mo (Control Mo), morphant embryos injected with 2 doses of *tbc1d32* Mo (10 ng or 15 ng). Scatter plots with bars represents the mean number of activated caspase 3+ cells per section for each condition, each dot corresponding to one embryo. Data are represented as mean ± SEM. Scale bar = 40 µm.

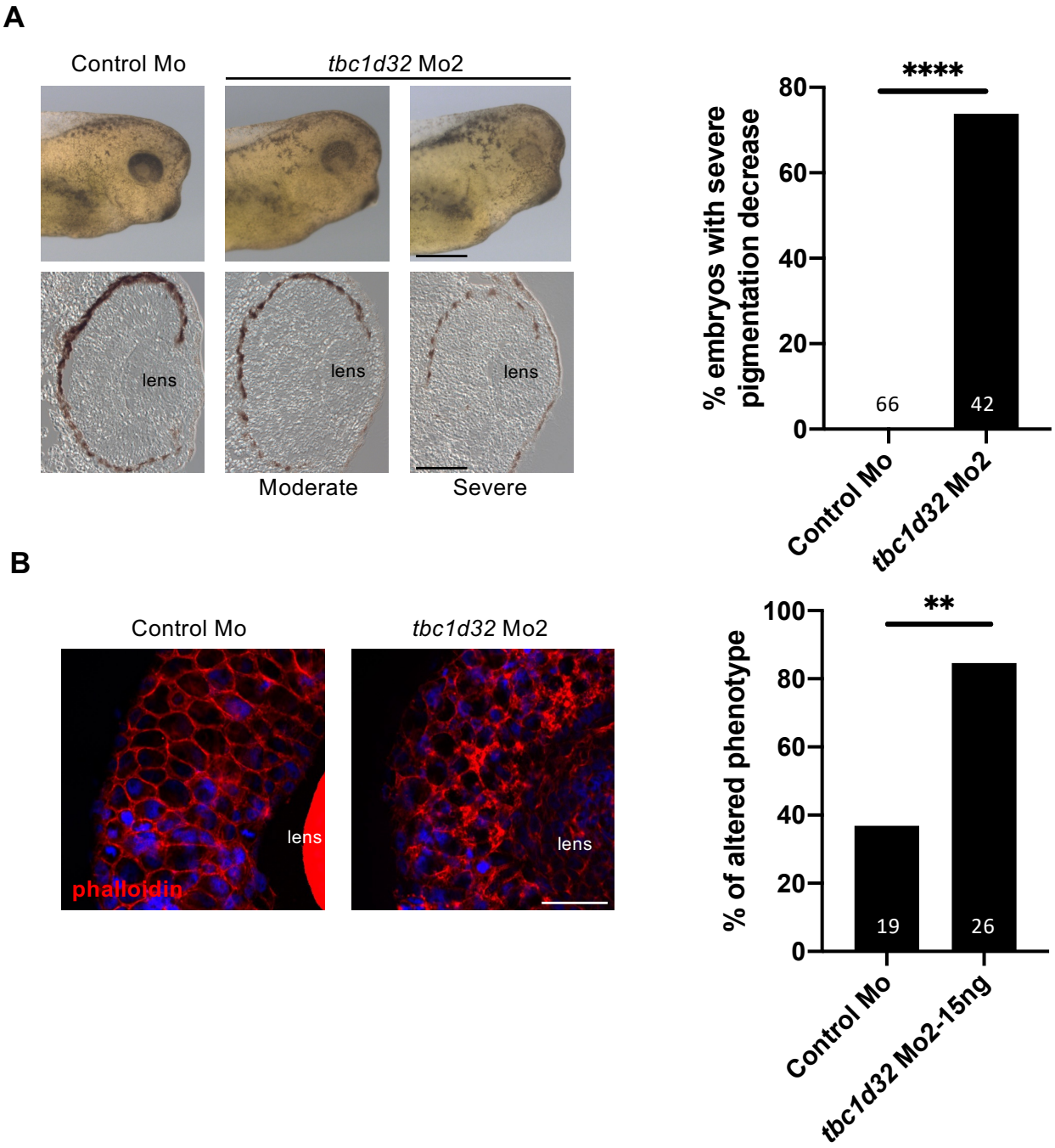

Supplemental Figure 6. *Xenopus* RPE phenotype in *tbc1d32* Mo2 injected embryos. A) Upper panels, lateral views of the head of one control and two morphant embryos with moderate and severe phenotypes (anterior to the right). Lower panels, transverse retinal sections of control and morphant embryos (dorsal side up). The histogram represents the percentage of embryos with a severe decrease in pigmentation among control (control Mo), and morphant (*tbc1d32* Mo2) groups. **B**) Phalloidin staining of filamentous actin on dissected eyes of control or Mo2 morphant *Xenopus* embryos at stage 35-36. The total number of embryos analyzed per condition is indicated in each bar. ****p<0.0001, **p<0.01; Fisher's exact test. Scale bars = 400 µm for whole mounts, 60 µm for sections in A, and 20 µm in B.

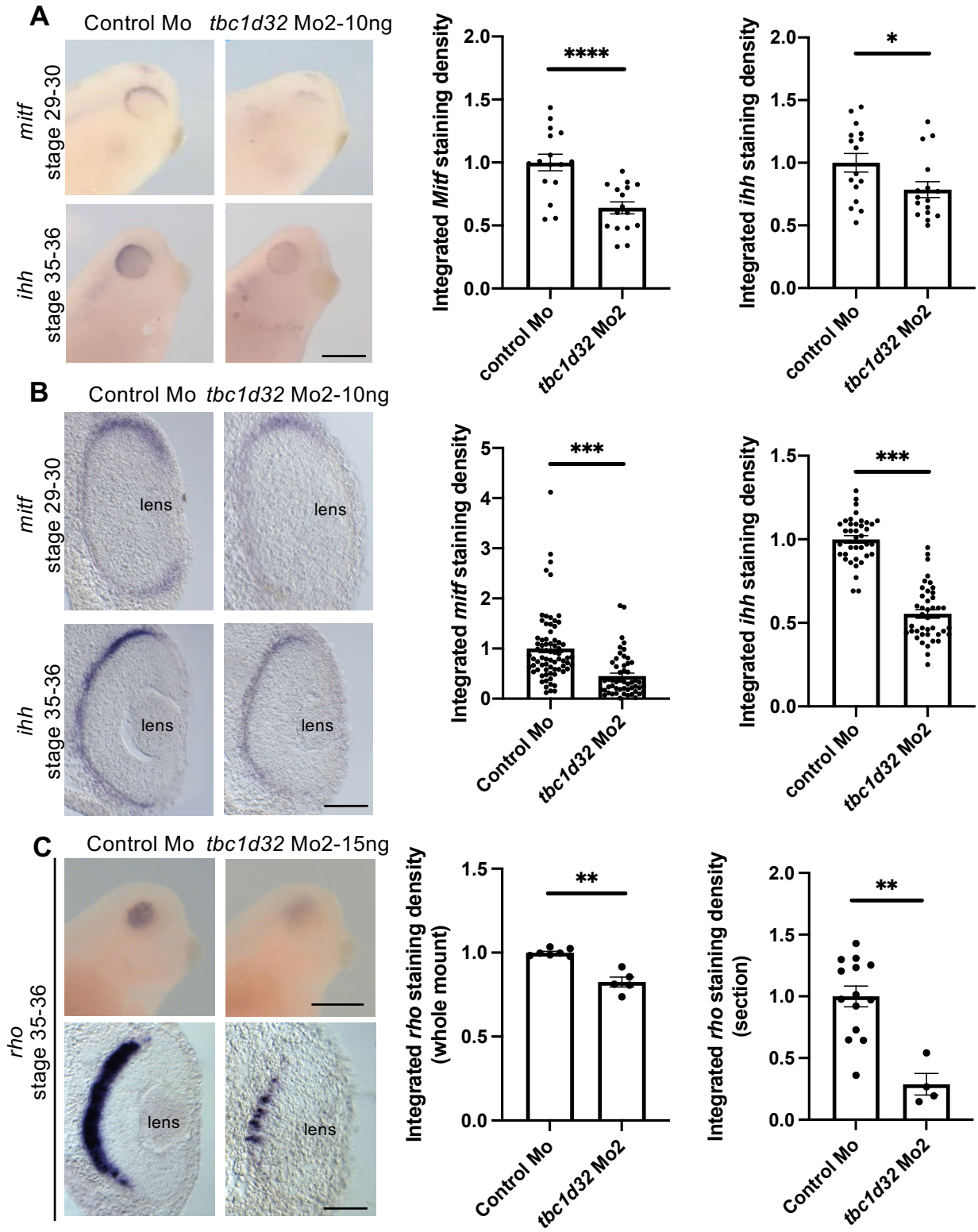

Supplemental Figure 7. *Xenopus* RPE marker expression following *tbc1d32* knockdown. A) Whole mount in *situ* hybridization against *mitf* or *ihh* on embryos injected with control Mo or *tbc1d32* Mo2 (lateral views of the head, anterior to the right). Scatter plots with bars represent quantification of the integrated density of *mitf or ihh* staining per eye relative to control Mo; each dot corresponds to one eye. **B)** Representative images of *mitf* or *ihh* staining on retinal sections of control or morphant embryos (dorsal side up). Scatter plots with bars represent quantification of integrated density of *mitf* or *ihh* staining relative to control Mo on retinal sections; each dot corresponds to one section. **C)** Upper panels, whole mount *in situ* hybridization against *rhodopsin* (*rho*) in embryos injected with control Mo or *tbc1d32* Mo2. Lower panels, transverse retinal sections of control and morphant embryos (dorsal side up). The scatter plots represent the quantification of the integrated density of *rho* staining relative to control Mo; each dot corresponds to one eye or one section. For all scatter plots, data are represented as mean ± SEM. *p<0.05; **p<0.01; ***p<0.001; ****p<0.0001; Mann and Whitney test. Scale bars = 400 µm for whole mounts and 40 µm for sections.

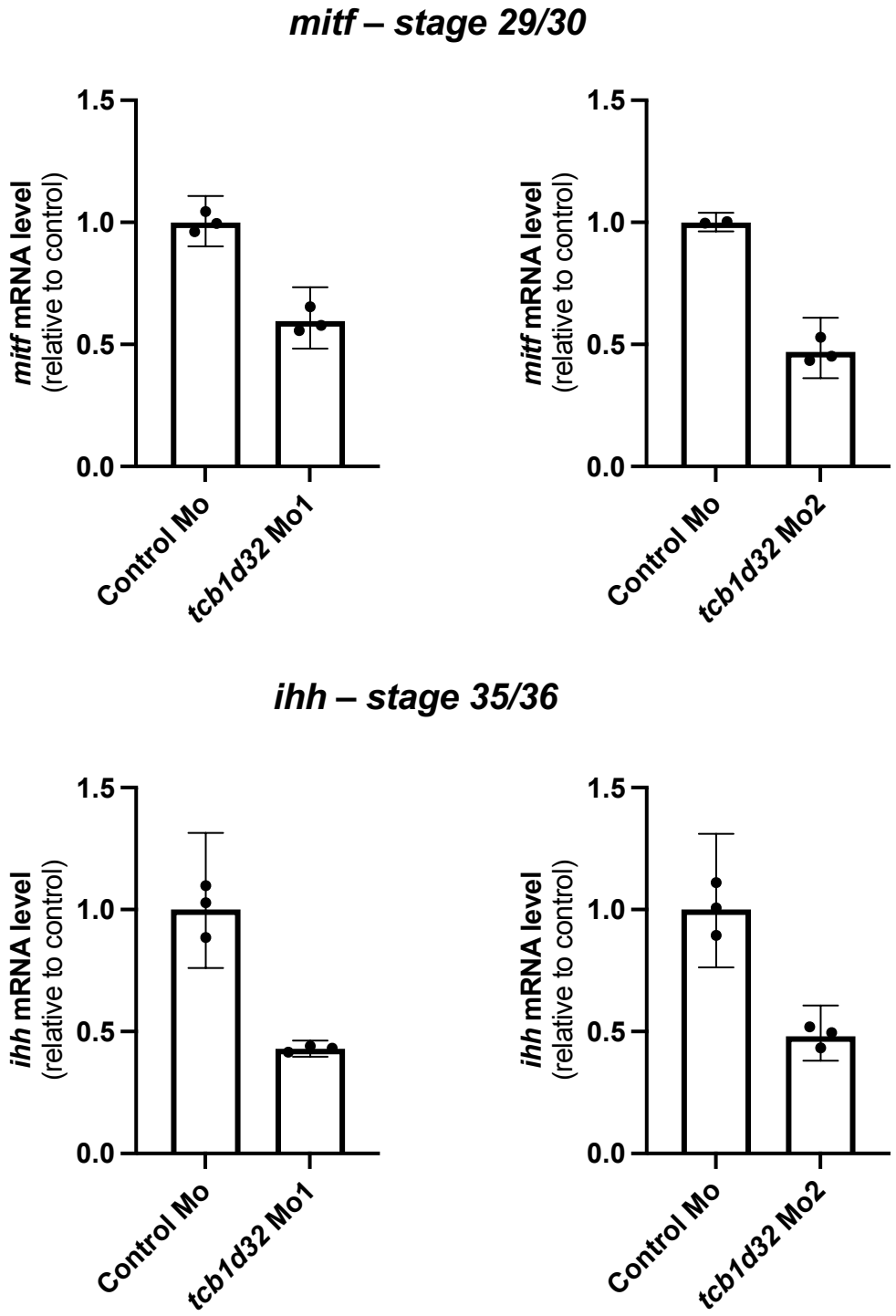

Supplemental Figure 8. *Xenopus* RPE marker expression following *tbc1d32* knockdown. qPCR analysis of *mitf* and *ihh* expression, in optic vesicles at stage 29-30 and whole eyes at stage 35-36, respectively, injected with control Mo, *tbc1d32* Mo1 or *tbc1d32* Mo2 (15ng). Data are represented as geometric mean with 95% CI; n = 3 technical replicates.

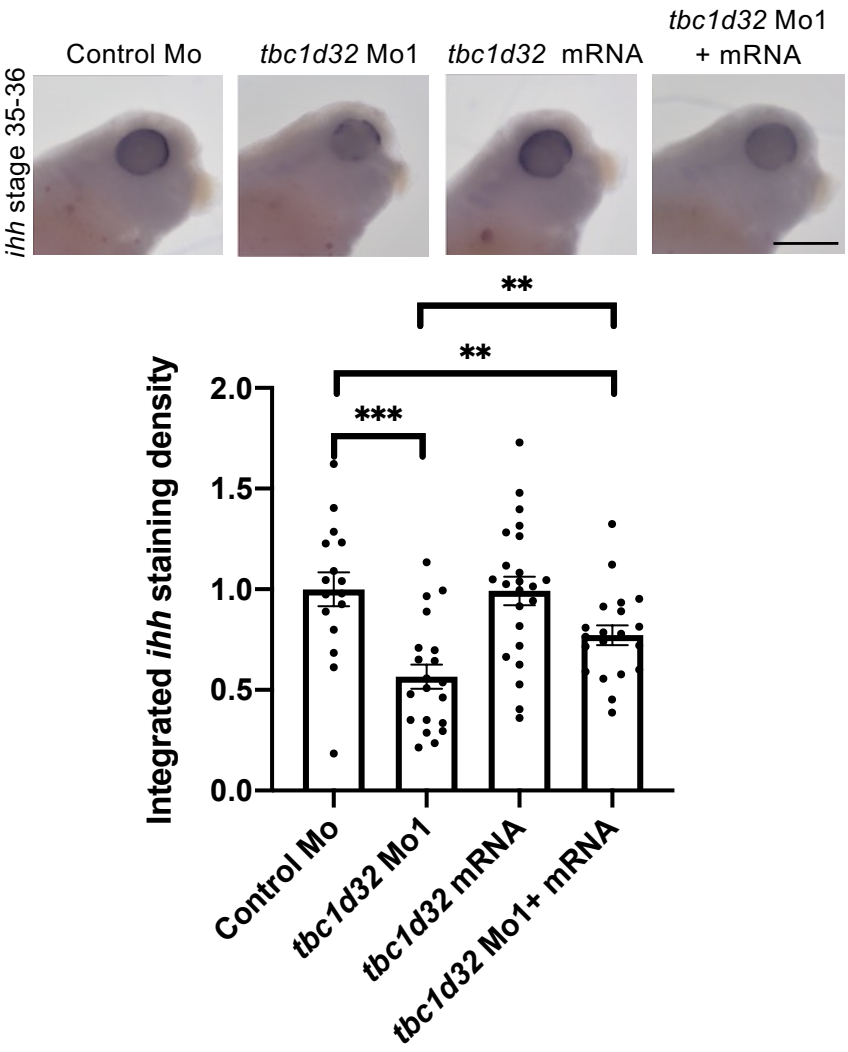

Supplemental Figure 9. *ihh* expression following *tbc1d32* Mo and mRNA co-injection. Whole mount *in situ* hybridization against *ihh* on stage 35-36 embryos injected with standard Mo, *tbc1d32* Mo1, *tbc1d32* mRNA, and *tbc1d32* Mo + *tbc1d32* mRNA (lateral view of the head, anterior to the right). Scatter plot with bars represents the quantification of *ihh* staining integrated intensity per eye relative to control Mo, each dot corresponding to one eye. Data are represented as mean ± SEM. **p<0.01; ***p<0.001; Mann and Whitney test. Scale bar = 400 μm.

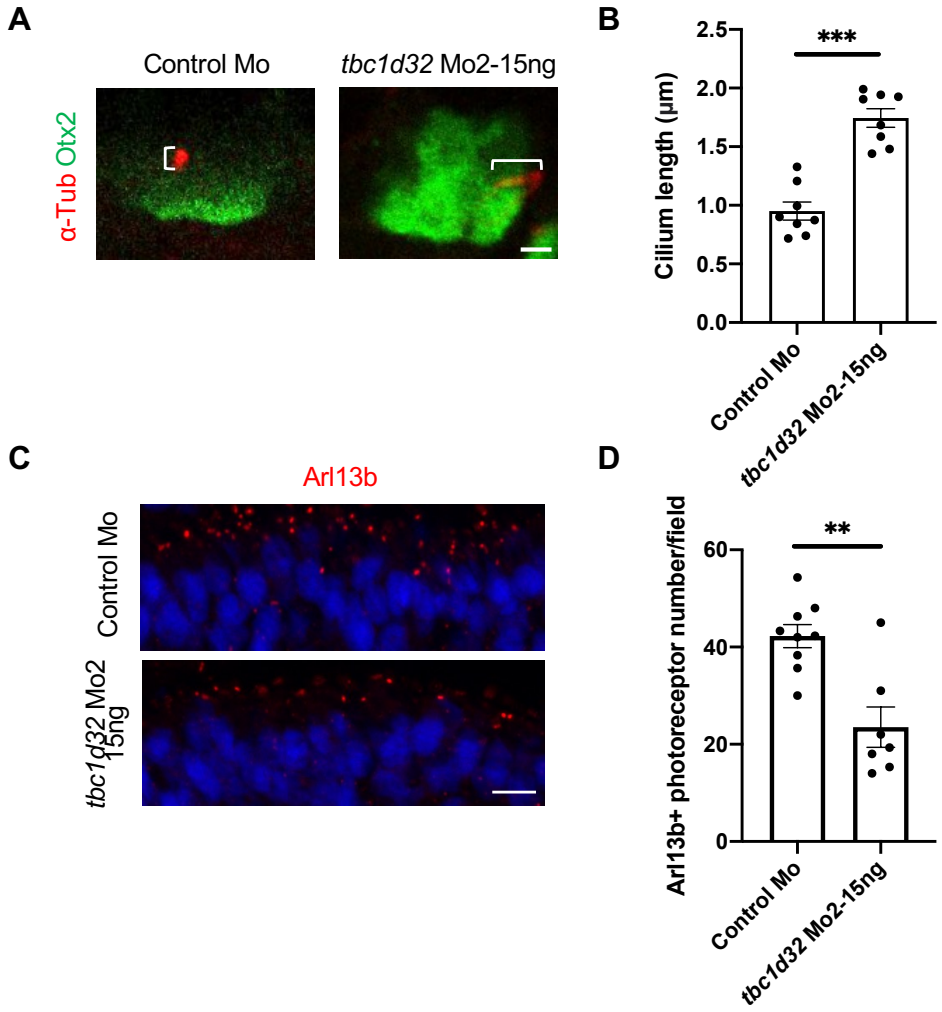

Supplemental Figure 10. Impact of *Xenopus* knockdown with *tbc1d32* Mo2 on retinal ciliogenesis. A) Immunolabelling of acetylated α-Tub and Otx2 showing a primary RPE cilium (delineated with brackets) on retinal sections of stage 35 embryos injected with a control Mo or with 15 ng of *tbc1d32* Mo2. **B)** Scatter plot with bars showing the mean cilia length in RPE cells. Each dot corresponds to the mean length for one embryo. **C)** Immunolabelling of Arl13b showing the photoreceptor connective cilium on retinal sections of stage 35 embryos injected with a control Mo or with 15 ng of *tbc1d32* Mo2. **D)** The scatter plot with bars shows the mean number of Arl13^{+} ciliated photoreceptors in one field of the central retina. Each dot corresponds to one embryo. All data are represented as mean ± SEM. **p<0.01, ***p<0.001; Mann and Whitney test. Scale bars = 2 µm in A and 20 µm in C.

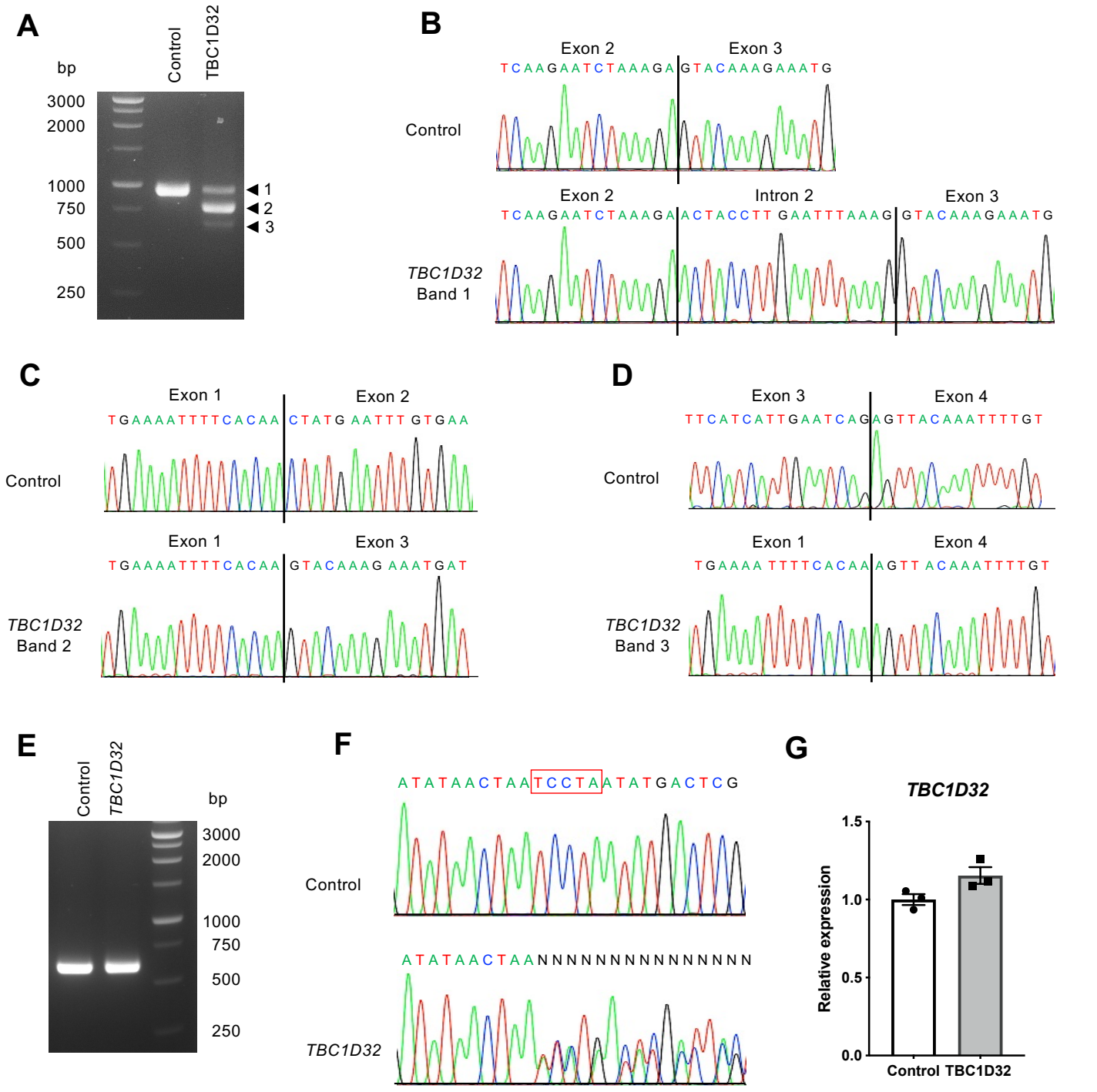

Supplemental Figure 11. Effect of *TBC1D32* variants carried by Patient 1 at the mRNA level. A) RT-PCR analysis of RNA isolated from control and Patient 1 fibroblasts using primers specific to exons 1 and 8 to further analyze the effect of the c.317+5G>A variant. A single amplicon of 931 bp is observed in control fibroblasts. Three amplicons of 949 bp (Band 1), 769 bp (Band 2) and 591 bp (Band 3) are observed in *TBC1D32* fibroblasts. **B**) Sequencing electropherograms (A, T, C, G) following subcloning of Band 1 shows the insertion of 18 bp of intron 2 between the exons 2 and 3 in comparison to the control sequence. **C**) Sequence electropherograms of Band 2 shows the skipping of exon 2 in comparison to the control sequence. **D**) Sequence electropherograms of Band 3 shows the skipping of exons 2 and 3 in comparison to the control sequence. The vertical lines in B, C and D represent the exon-intron junctions. **E**) RT-PCR analysis of RNA isolated from control and Patient 1 fibroblasts using primers specific to exons 6 and 11 to assay the effect of the c.846delTCCTA variant. A single amplicon of 604 bp is observed in control and *TBC1D32* fibroblasts. **F**) Sequence electropherograms show the deletion of the TCCTA sequence (boxed in red) and subsequent frameshift in *TBC1D32* fibroblasts as compared to controls. **G**) qPCR analysis of *TBC1D32* expression levels in control (black bars) and *TBC1D32* (grey bars) fibroblasts. Data are represented as mean ± SEM.

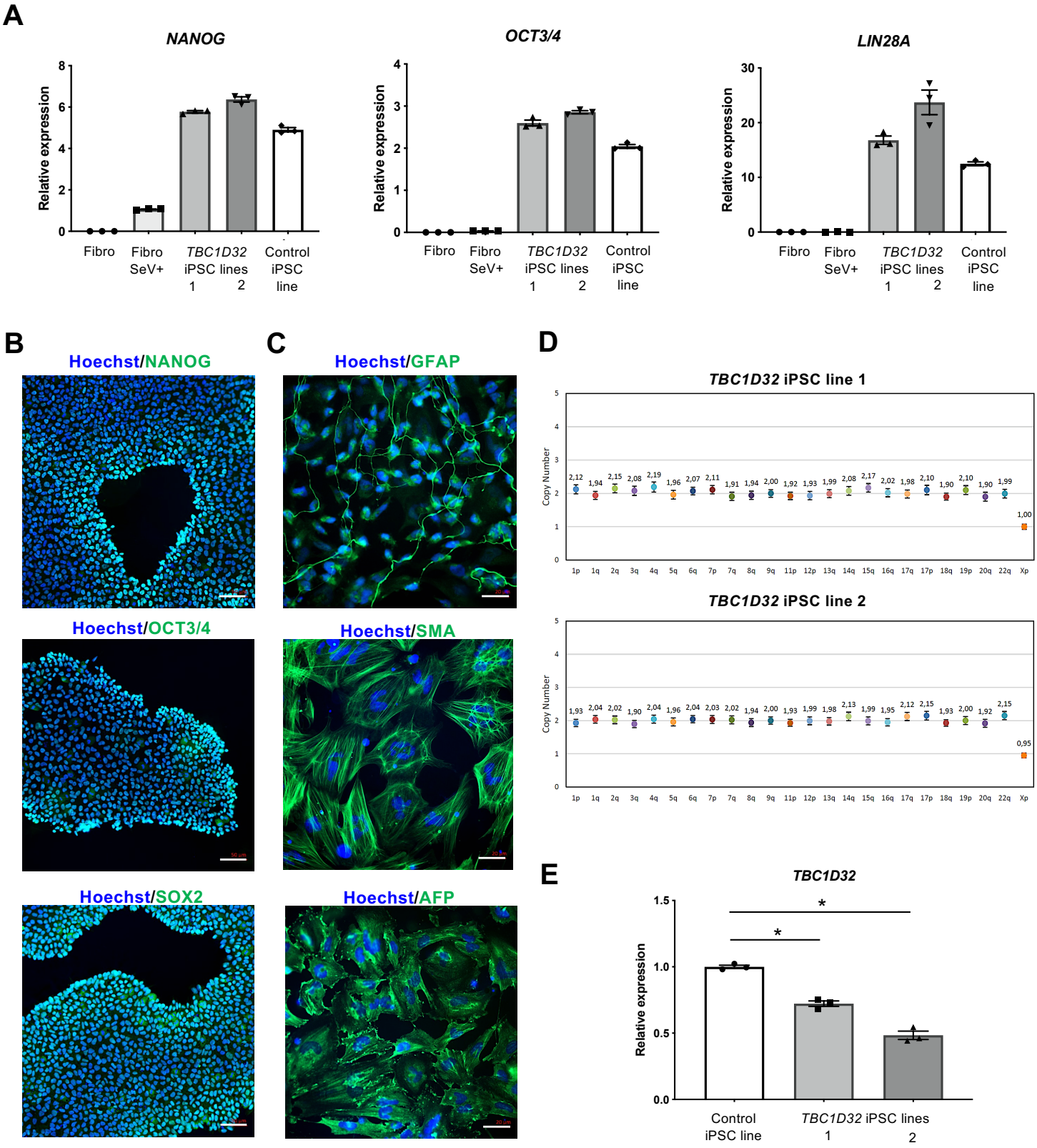
A
NANOG
OCT3/4
LIN28A
Relative expression
Fibro
Fibro SeV+
TBC1D32 iPSC lines 1 2
Control iPSC line
B
Hoechst/NANOG
Hoechst/OCT3/4
Hoechst/SOX2
C
Hoechst/GFAP
Hoechst/SMA
Hoechst/AFP
D
TBC1D32 iPSC line 1
TBC1D32 iPSC line 2
Copy Number
E
TBC1D32
Relative expression
F
TAAAGAGTGAGTATGGCCATA
TAAAGAGTGAGATATGGCCATA
ATATAACTAATCCTAATATGA
ATATAACTAA NNNNNNNNNNN
Control iPSC line
c.317+5G
TBC1D32 iPSC line 1
c.317+5G>A
Control iPSC line
c.846TCCTA
TBC1D32 iPSC line 1
c.846delTCCTA

Supplemental Figure 12. Quality controls of *TBC1D32* iPSC lines from Patient 1. A) qPCR analysis of the pluripotency markers *NANOG*, *OCT3/4* and *LIN28A* in fibroblasts, fibroblasts transduced with Sendai reprogramming vectors (Fibro SeV+; light grey bars), *TBC1D32* iPSC lines 1 and 2 (dark grey bars), and a control iPSC line (black bars). Data are represented as mean ± SEM. **B**) IF analysis of the pluripotency markers NANOG, OCT3/4 and SOX2 (in green; nuclei labelled in blue) in *TBC1D32* iPSC line 1. Scale bars = 70 µm. **C**) IF analysis of the germline markers glial fibrillary acidic protein (GFAP; ectoderm), smooth muscle actin (SMA; mesoderm) and alpha-fetoprotein (AFP; endoderm), following EB differentiation of *TBC1D32* iPSC line 2. Scale bars = 40 µm. **D**) Digital qPCR analysis of rearrangement hotspots in *TBC1D32* iPSC lines showing a copy number of 2 for all autosomal regions, and a copy number of 1 for the X chromosome. **E**) qPCR analysis of *TBC1D32* expression in *TBC1D32* iPSC lines (grey bars) in comparison to a control line (black bar). Data are represented as mean ± SEM; n = 3 technical replicates; $p<0.05$; Mann and Whitney. **F**) Sanger sequencing of the regions carrying the variants c.317+5G>A and c.846delTCCTA (red boxes) in the *TBC1D32* iPSC line 1 in comparison to a control iPSC line.

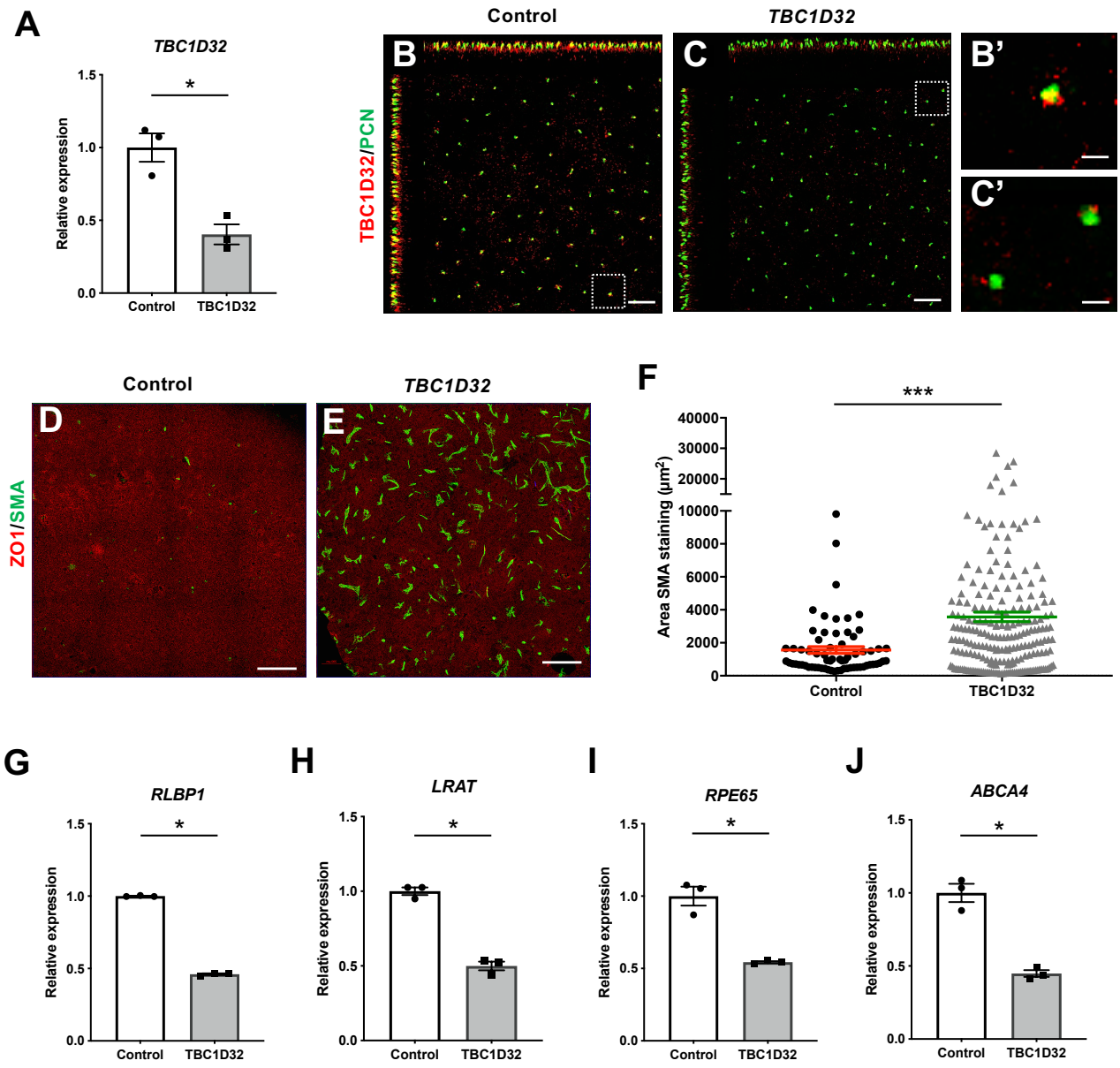

Supplemental Figure 13. Expression of *TBC1D32* and EMT and visual cycle markers in iPSC-derived RPE. A) qPCR analysis of *TBC1CD32* expression in control (black bar) and patient (grey bar) iPSC-derived RPE. Data are represented as mean ± SEM; n = 3 technical replicates; $p<0.05$; Mann and Whitney. IF studies and MIP confocal imaging of TBC1D32 and PCN expression in control (**B**) and *TBC1D32* (**C**) iPSC-derived RPE. Scale bars = 10 µm **B'**, **C'**) Higher magnification of the boxed cells shown in B (scale bar = 2 µm) and C (scale bar = 2.5 µm), respectively. **D**) A 16 field-montage of a transwell filter of control (**D**) and *TBC1D32* (**E**) iPSC-derived RPE immunolabelled for ZO1 and SMA. Scale bars = 50 µm. **F**) Scatter plot represents the quantification of each area of SMA staining in control (n = 67) and *TBC1D32* (n = 230) iPSC-derived RPE shown in D and E. Data are represented as mean ± SEM; ***$p<0.0005$; Student's t-test. qPCR analysis of the visual cycle markers *RLBP1* (**G**), *LRAT* (**H**), *RPE65* (**I**) and *ABCA4* (**J**) in control (black bar) and patient (grey bar) iPSC-derived RPE. Data are represented as mean ± SEM; n = 3 technical replicates; *$p<0.05$; Mann and Whitney.